A New Proposal to Jefferson Lab PAC-25

Measurement of G_E^p/G_M^p using elastic $\vec{p}(\vec{e}, e')p$ up to $Q^2 = 3.50$ (GeV/c)^2

December 2, 2003

J. Arrington, K. Hafidi, R.J. Holt, H.E. Jackson, D.H. Potterveld,
P.E. Reimer, E.C. Schulte, B. Zeidman, X. Zheng[1] (co-spokesperson)
Argonne National Laboratory, Argonne, IL 60439

J.-P. Chen, R. Ent, D. Gaskell, D. Higinbotham, D. Mack, B. Reitz
Thomas Jefferson National Accelerator Facility, Newport News, VA 23606

S. Širca
University of Ljubljana, Slovenia

W. Bertozzi, O. Gayou, S. Gilad, P. Monaghan, Y. Qiang, L. Wan, Y. Xiao, C. Zhang
Massachusetts Institute of Technology, Cambridge, MA 02139

Z.-L. Zhou
Schlumberger-Doll Research, Ridgefield, CT 06877

W. Hersman, J.R. Calarco (co-spokesperson), M. Holtrop, T. Lee, H.-G.Zhu
University of New Hampshire, Durham, NH 03824

R. Segel, I. Qattan
Northwestern University, Evanston, IL 60208

D.V. Jordan, J.I. McIntyre, B.D. Milbrath, G. Warren
Pacific Northwest National Lab, Richland, WA 99352

R. Gilman, X. Jiang, K. McCormick
Rutgers, The State University of New Jersey, Piscataway, NJ 08855

S. Choi, Z.-E. Meziani
Temple University, Philadelphia, PA 19122

G.D. Cates, D.G. Crabb, D. Day, N. Liyanage, P. Mckee,
O.A. Rondon (co-spokesperson), J. Singh, W.A. Tobias, F. Wesselmann
University of Virginia, Charlottesville, VA 22904

[1]contact person, email: xiaochao@jlab.org

Abstract

We propose here measurements of the ratio G_E^p/G_M^p via doubly polarized elastic $\vec{p}(\vec{e},e')p$ scattering at $Q^2 = 2.10$ and 3.50 (GeV/c)^2. The UVa polarized NH_3 target will be used in Hall C with its spin aligned $139°$ w.r.t. the beam direction. To extract G_E^p/G_M^p, we perform single-arm electron scattering measurements at kinematics where the elastic asymmetries are the most sensitive to this ratio. In addition, the asymmetry will be measured at $Q^2 = 0.61$ (GeV/c)^2 to determine the absolute electron beam helicity state and to check the product of beam and target asymmetries. Assuming 80% beam polarization and 85 nA current, we request 14 days of beam time to achieve a precision of $\Delta(\mu G_E^p/G_M^p) = 0.057$ and 0.074 at $Q^2 = 2.10$ and 3.50 (GeV/c)^2, respectively. Here $\mu = \mu_p$ is the proton magnetic moment. We request 3 days overhead time.

The proposed measurement will provide the first data of G_E^p/G_M^p from the $\vec{p}(\vec{e},e')p$ asymmetry method in the range $Q^2 > 2$ (GeV/c)^2 with good precision. It represents the next step in a logical scientific progression to fully understand the discrepancy between data from the Rosenbluth separation and the polarization transfer technique. One possible explanation of this observed discrepancy is the two-photon exchange correction, which so far is difficult to study experimentally. The direct extraction of G_E^p/G_M^p from the double polarization asymmetry is expected to be less sensitive to the two-photon exchange effect than the Rosenbluth separation. Moreover, calculations on the two-photon exchange correction need more development and will probably use the observed discrepancy itself as an input. While based on the same double polarization principles, the new method has completely different systematic uncertainties than the polarization transfer method. Especially, it does not suffer from the uncertainties due to spin precession. Hence it will provide an independent check of the polarization transfer data before spending extensive effort on studying the two-photon exchange effect. Finally, in addition to the two-photon exchange, there might be other processes we are not aware of, that can cause the discrepancy. The new data will give an opportunity to explore such unknown effects.

Contents

1 Motivation **4**
1.1 Theories . . . 4
1.2 Existing Data . . . 4
1.3 Two-Photon Exchange Correction . . . 6

2 The Proposed Experiment **7**

3 Experimental Setup **7**
3.1 Overview . . . 8
3.2 Beam Line . . . 8
3.3 The UVa NH_3 Target . . . 9
3.4 Spectrometer . . . 12
3.5 Acceptance Effect due to Target Magnetic Field . . . 13
3.6 Low Q^2 Measurement . . . 13
3.7 Data Analysis . . . 14

4 Expected Uncertainties and Rate Estimation **14**
4.1 Experimental Systematics . . . 14
4.2 Beam Charge Asymmetry . . . 14
4.3 Target Polarization . . . 14
4.4 Target Dilution Factor . . . 15
4.5 Nitrogen Asymmetry . . . 16
4.6 Background . . . 17
4.7 Electromagnetic Radiative Corrections . . . 17
4.8 Deadtime Correction . . . 17
4.9 Optimization of Kinematics . . . 17
4.10 Summary of Rate and Expected Uncertainties . . . 19

5 Beam Time Request **21**

6 Comparison to Other Methods **21**
6.1 Comparison to Coincidence and Single-Proton Measurement . . . 21
6.2 Comparison to PR01-105 . . . 22

7 Summary **22**

A Doubly Polarized Elastic Scattering **23**

B Error Propogation of Systematic Uncertainties for G_E^p/G_M^p **24**

C PAC-20 report for PR01-105 **26**

1 Motivation

The nucleon is one of the basic building blocks of nature. The elastic form factors are important fundamental properties of the nucleon, describing its internal structure due to the spatial distribution of its charge and magnetism, and play an essential role in hadronic physics as the *sine qua non* input to our understanding of the nucleon structure. Thus it is of the utmost urgency that we have accurate and reliable measurements of these fundamental characteristics of the nucleon from low Q^2 to the highest Q^2 we can reach. However, there is a discrepancy between the proton G_E/G_M data obtained by two very different techniques that clearly indicates a problem in either the experimental methods or the theoretical basis used to extract the form factors from the data. Any such discrepancies must be resolved without delay. In this proposal, we propose an independent measurement of the ratio G_E/G_M on the proton using a third technique which is experimentally unrelated to either of the first two. In the following we will first briefly review available calculations for G_E^p/G_M^p, then give an overview of previous world data and propose a new method to measure this ratio.

1.1 Theories

The proton elastic form factors have been calculated in various models. At low four momentum transfer squared $Q^2 < 1$ (GeV/c)^2, the Vector Meson Dominance (VMD) model [1] successfully describes the nucleon form factors. In the high Q^2 region, the dominant degrees of freedom of the nucleon are the three valence quarks and perturbative Quantum Chromo-Dynamics (pQCD) can be applied [2]. Specifically, based on the leading-order pQCD, or hadron helicity conservation, the ratio of Dirac and Pauli form factors F_2^p/F_1^p is expected to scale as $1/Q^2$ at high Q^2 [2, 3], which directly constrains the behavior of G_E^p/G_M^p in this region.

In the intermediate region $1 < Q^2 < (10 - 20)$ (GeV/c)^2 (or higher), however, predictions for the nucleon form factors become difficult because the soft scattering processes are still dominant compared to hard scattering. Moreover, these soft contributions might be different for different observables of the scattering processes. This fact itself can be used as a tool to understand the role of the soft processes without reaching asymptotically high Q^2. Many QCD models have been used to calculate the elastic nucleon form factors in this region - the relativistic constituent quark model (RCQM) [4, 5], the cloudy bag model (CBM) [8], the SU(6) breaking CQM [7], the point-form spectator approximation (PFSA) model based on the Goldstone boson exchange CQM [6], and the chiral soliton model [9]. Figure 1 shows existing calculations for $\mu G_E^p/G_M^p$ along with existing world data, where $\mu = \mu_p = 2.793\mu_N$ is the proton magnetic moment.

1.2 Existing Data

The proton elastic form factors have been measured for almost five decades. In the traditional Rosenbluth separation method, based on the assumption of the one photon exchange process, the elastic cross section is measured at fixed Q^2 but different values of the virtual photon polarization ε. Then the values of G_E^p, G_M^p and their ratio are extracted from a linear fit of the cross section as a function of ε. This method is usually used at $Q^2 < 9$ (GeV/c)^2. Data from this method show that G_M^p can be approximated by the dipole form $G_D = \mu/(1 + Q^2/0.71)^2$, at least up to about $Q^2 = 3 - 4$ (GeV/c)^2. The ratio $\mu G_E^p/G_M^p$ is observed by this method to be close to unity. Above this Q^2 region, G_M^p is extracted from single cross section measurements assuming $\mu G_E^p = G_M^p$. Data on F_1^p at $Q^2 > 10$ (GeV/c)^2 show a $1/Q^4$ scaling behavior which is consistent with pQCD predictions [10].

However, recent data from the method of measuring the polarization transfer [12, 13, 14] showed that $\mu G_E^p/G_M^p$ drops linearly as Q^2 increases and reaches as low as ≈ 0.3 at $Q^2 = 5.6$ (GeV/c)^2, in significant disagreement with the Rosenbluth data (see Fig. 1). This dramatic change has provoked large

Figure 1: Previous world data for $\mu G_E^p/G_M^p$ from a global analysis of Rosenbluth data [11] (open squares) and from polarization transfer method [12, 13, 14] (open and solid stars). A dramatic disagreement is clearly seen between the two data sets at $Q^2 > 2$ (GeV/c)^2. Preliminary results (not shown) from a recent Hall A high precision Rosenbluth experiment [18] agree well with Rosenbluth data. Curves are calculations from VMD (black) [1], RCQM (red) [5], PSFA (green) [6], SU(6) breaking with CQM FF (blue) [7] and chiral soliton model (magenta) [9].

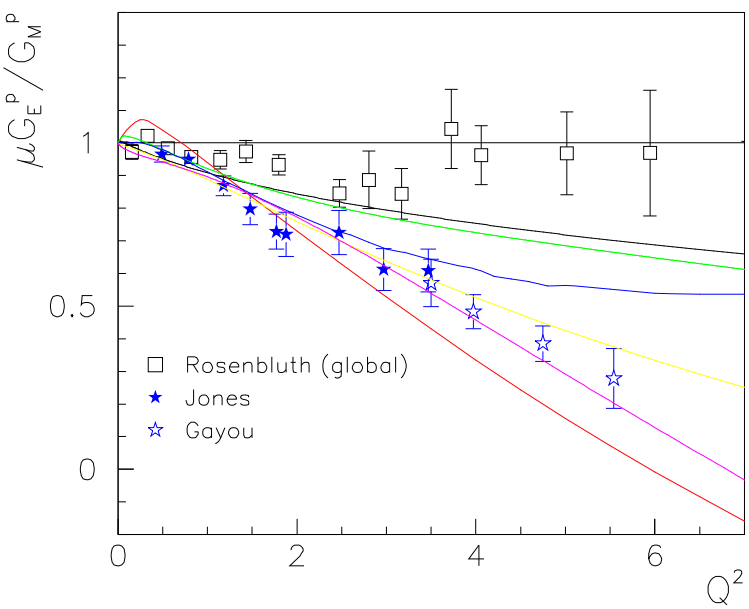

interest in both theoretical and experimental aspects of the proton form factor studies. Different fits have been performed separately to cross section data, and data from both cross section measurements and polarization transfer methods [17]. Previous Rosenbluth data have been re-analyzed [15] but the results are still inconsistent with polarization measurements. At high Q^2, data from cross section measurements have also been re-analyzed [15] using the polarization transfer fit [13].

Experimentally, preliminary results from the recently completed Hall A high precision Rosenbluth experiment E01-001 [18] agree well the traditional Rosenbluth data. A new polarization transfer experiment [19] is planned in Hall C to measure $\mu G_E^p/G_M^p$ via polarization transfer up to $Q^2 = 9.0$ (GeV/c)^2. Since a new proton polarimeter will be used, it is expected to check the systematic uncertainties of previous polarization transfer data, especially those due to the uncertainty of the spin precession. However the new experiment is still based on the same technique and analyzing methods as previous polarization transfer experiments, so it will still share some of the systematics. Therefore, it is important to have a fully independent double polarization experiment, and this is *the* main purpose of this proposal.

1.3 Two-Photon Exchange Correction

In order to explain the discrepancy between the Rosenbluth separation and polarization transfer data, assuming that both are correct, significant effort has been spent on the understanding of radiative corrections and soft processes that can modify the results obtained under the assumption of one-photon exchange. The validity of radiative corrections has been checked, and it has been suggested that the two-photon exchange process may explain part of the discrepancy between the two data sets.

Earlier data on the ratio of the $e^+ - N$ and $e^- - N$ scattering cross sections indicate that the two-photon exchange correction is small [20]. As a result, when analyzing the Rosenbluth data, the two-photon (and higher order) exchange corrections are small in the traditional radiative corrections [21]. This correction can introduce an ε-dependence to the cross section and effect the linearity of the Rosenbluth plot. Guichon and Vanderhaeghen [22] showed that, based on general forms of this correction, the effect on the Rosenbluth data is much larger than that on the polarization transfer data, and the true $\mu G_E^p/G_M^p$ is about 20% below the fit to polarization transfer data. Blunden, Melnitchouk and Tjon [23] evaluated the two-photon exchange contributions to elastic $e - p$ scattering cross sections based on a simple hadronic model including the finite size of the proton. Their results explained one third of the discrepancy between the two data sets.

Rekalo and Tomasi-Gustaffson [24] derived from first principles, *i.e.* the C-riance of the EM interaction and the crossing symmetry, the general properties of two-photon exchange in $e - p$ elastic scattering. They showed that the presence of this mechanism destroys the linearity of the Rosenbluth separation but does not significantly affect the terms related to the EM form factors.

In this context, it is important to note that the ratio $\mu G_E/G_M$ will also affect the extraction of G_M from cross section data. Previous work by Brash *et al.* [25] showed that, if a fit to the polarization transfer data is used to reinterpret the Rosenbluth separations, it will result in a slightly larger magnetic form factor than previously inferred. While they offer no physical explanation, this is precisely the direction to simulate the two-photon exchange calculation.

Armed with the prediction that the two-photon exchange could be large, earlier SLAC data on the ratio of the $e^+ - p$ and $e^- - p$ scattering cross sections have been re-examined to see if the two-photon exchange effects on the cross section may explain the discrepancy in $\mu G_E^p/G_M^p$ data. It has been shown that there is indeed a hint that the two-photon exchange correction is large [26]. However the e^+ data were obtained in a low Q^2 region ($Q^2 \lesssim 2$ (GeV/c)^2) and are not precise enough to set a good limit on this correction for higher Q^2. It is interesting to see how people's opinion changes with time – what we believed forty years ago turn out to be incorrect and those important measurements (e^+ scattering in this case) were abandoned just because they were *supposed* to give the same results as other measurements (e^- scattering).

The polarization transfer experiment, on the other hand, provide a more direct measurement of the ratio $\mu G_E/G_M$. The calculations show that the two-photon contributions to the electric and magnetic components are small to moderate, and in the same direction, but not equal [22, 23, 27]. Therefore, while the ratio $\mu G_E/G_M$ from the spin transfer measurement will be affected by the two-photon exchange contributions, the size of the effect is expected to be much less than for the Rosenbluth separation technique and maybe within experimental uncertainties for the higher Q^2 data points. The same is true for the asymmetries of doubly polarized elastic scattering.

Experimental study of the two-photon exchange effect is possible. In fact, it has been predicted [28, 29] that the interference between the one- and two-photon exchange processes leads to a non-zero asymmetry A_N for target polarized transversely to the scattering plane. An early attempt to measure this at SLAC showed the asymmetry to be zero but within rather large errors [30]. There has been a recent suggestion to measure this asymmetry using BLAST at the MIT-Bates accelerator facility, and a proposal is

also being prepared for Hall C [31]. Other possibilities include the transverse beam asymmetry A_y. Such data exist at very low Q^2, around 0.1 (GeV/c)^2, from the MAINZ-A4 and the SAMPLE experiments [32]. However, such direct measurements of the two-photon exchange are usually very difficult, they require very high precision data on either cross sections (Rosenbluth linearity check), or on asymmetries (A_T) over a wide kinematic (ε) range. Or, a facility development is required (transversely polarized target for A_N, or special designed polarimeter for P_N).

The two-photon exchange correction provides a possible explanation of the discrepancies in the existing data. Furthermore it not only affects the extraction of form factors from $e-p$ scattering, but also affects many other observables, *e.g.* parity-violating asymmetries. A full understanding of this process may take many years, and a large amount of experimental study is necessary to provide guidance to theoretical work. We also cannot exclude the possibility that there might be other corrections of which we are not aware of, that add to the discrepancy between the two form factor data sets. Hence it might not be appropriate to attribute the full discrepancy to two photon exchange effects. In this sense, it is more than necessary to perform an independent determination of $\mu G_E/G_M$ from double polarization observables to check the results from the polarization transfer data, before significant efforts are spent on the study of two-photon exchange effects.

2 The Proposed Experiment

We propose here a third method to measure G_E^p/G_M^p in the intermediate Q^2 range at 2.10 and 3.50 (GeV/c)^2. We will measure the double polarization asymmetry in $\vec{e}-\vec{p}$ elastic scattering and the G_E^p/G_M^p ratio will be extracted from the measured asymmetries. Formulas for doubly polarized elastic scattering and its asymmetries are given in Appendix A. The UVa polarized NH_3 target will be used in Hall C with its spin aligned at 139° w.r.t. the beam-line (*i.e.* pointing to the left of the beam-line when viewing toward beam dump). The scattered electrons will be detected in the HMS. In addition, the asymmetry at $Q^2 = 0.61$ (GeV/c)^2 will be measured with a statistical uncertainty of 2%, which will serve to determine the absolute electron helicity state and to check the product of beam and target polarizations.

Assuming 85 nA beam current with 80% polarization, we request 14 days beam time to reach an uncertainty $\Delta(\mu G_E^p/G_M^p) = 0.057$ and 0.074 at $Q^2 = 2.10$ and 3.50 (GeV/c)^2, respectively. Three days overhead time are needed for beam pass change and target work.

The proposed measurement will provide the first precision data on $\mu G_E^p/G_M^p$ from a third method in the intermediate Q^2 range. This method is expected to be less sensitive to the two-photon exchange effect than Rosenbluth separation, based on the same argument as for the polarization transfer, *i.e.* it is a direct measurement of $\mu G_E^p/G_M^p$. Furthermore, it has different systematic uncertainties compared to the polarization transfer technique. Hence, it will complement these two methods. The new results will provide crucial information on both the proton structure and the understanding of previous world data, and provide reliable guidance for theoretical work on two-photon exchange corrections.

3 Experimental Setup

In the following we describe the experimental setup for the proposed measurement in Hall C.

3.1 Overview

The floor plan for Hall C is shown in Fig. 2. The UVa polarized NH_3 target will be installed with its spin direction aligned at 139° w.r.t. the beam-line, as shown in Fig. 3. The scattered electrons will be detected by the HMS. Elastic events are identified by the electron scattering angle and momentum with elastic kinematic conditions.

Figure 2: Hall C floor plan for the proposed measurement (not to scale).

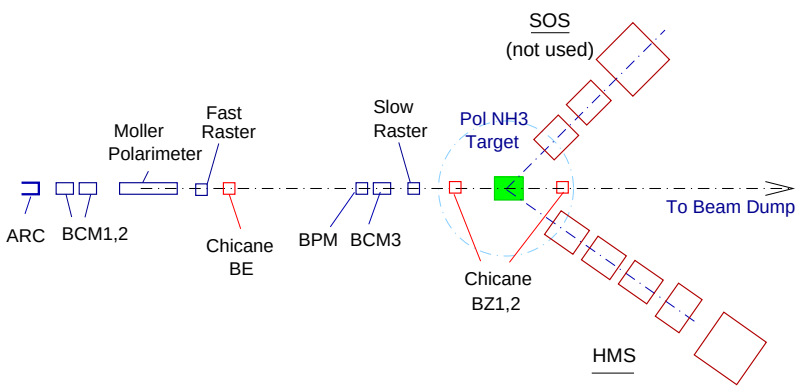

Figure 3: Kinematics for the proposed measurement. Target spin angles are shown for the case when scattering plane is horizontal ($\phi^\star = 0°$).

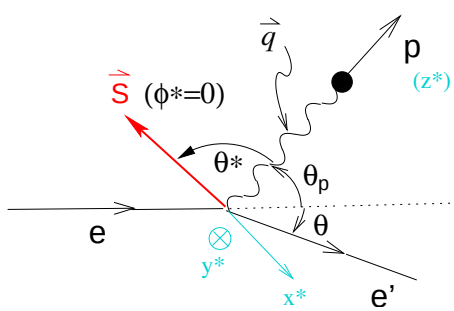

3.2 Beam Line

We propose to use polarized electrons with 80% polarization and 85 nA beam current at two beam energies 3.60 and 6.00 GeV. Beam energy will be measured to $\Delta E/E = 5 \times 10^{-4}$ level using the ARC method [33]. We plan to use the Møller polarimeter for beam polarization measurement. Currently the Hall C Møller polarimeter can provide better than 1% precision. However additional systematic error can come from the fact that we are running at 85 nA. We therefore use 1.5% in the uncertainty estimation.

Because the target spin is not parallel to the beam direction, the strong 5 T magnetic field of the target

Figure 4: Hall C beam line chicane magnets and raster system. The BZ2 magnet and the beam-line downstream of the target will be replaced by a He bag.

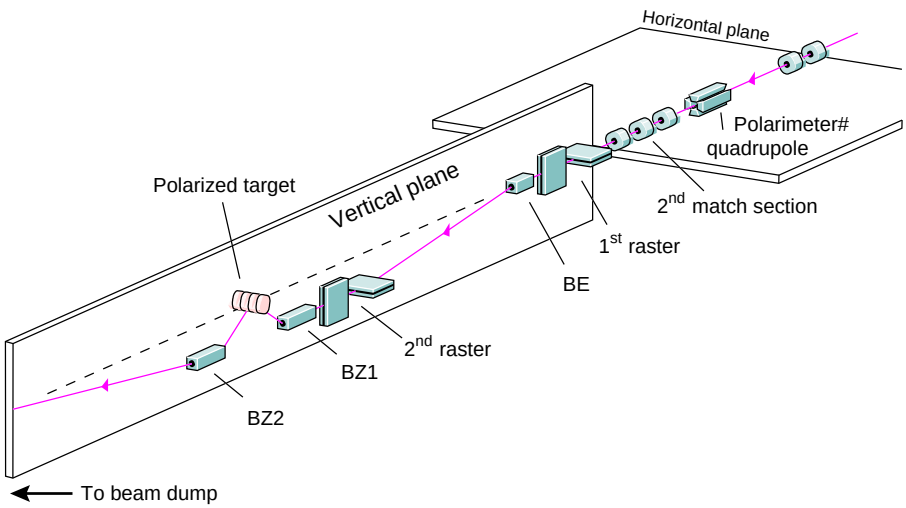

will bend the electron beam toward the floor. In order to ensure that the incoming beam is incident on the target cell horizontally, we will use Hall C's BE and BZ1 chicane magnets to bend the beam up before it enters the target scattering chamber. A downstream chicane magnet will not be used. Instead a He bag will be used for transporting the beam downstream of the target to the beam dump. A series of chicane magnets were used for a similar purpose during the G_E^n experiment E93-026 [35] and the Resonance Spin Structure E01-006 [37], and we will use the same setup.

The beam needs to be rastered to maintain the target polarization and to ensure uniform distribution of both heat and radiation on the target material. We require the beam spot at the target to be ≈ 2 cm in diameter which almost covers the entire target. This has been achieved during previous experiments [35, 37] using the slow rastering system. A schematic diagram for the beam-line chicane magnets and raster system is shown in Fig. 4.

Beam position monitoring and beam current measurement at our low current of 85 nA need special care. Using the same Secondary Emission Beam Position Monitor (SEM) [38] as in previous experiments E93-026 and E01-006, we believe a precise beam position monitoring can be achieved. An upgrade of the SEM electronics to operate in updating mode at the 30 Hz beam helicity flip rate is desirable, but not required. The beam current can be measured to a level of 5%. The effect of beam charge asymmetry will be discussed in Section 4.2.

3.3 The UVa NH_3 Target

We will use a solid polarized proton target developed by the University of Virginia. For the proposed measurement, the target material is $^{15}NH_3$. In this target, Dynamic Nuclear Polarization (DNP) is utilized to enhance the low temperature (≈ 1 K), high magnetic field (5 T) polarization of solid materials. The irradiation of the target with 140 GHz microwaves drives hyperfine transitions which align the nucleon spins. This target was successfully used in the SLAC experiments E143, E155, E155x and two experiments E93-026 [35] and E01-006 [37] in Hall C. The proton polarization in $^{15}NH_3$ can reach as

high as 95% and will decrease because of beam induced radiation damage. An average polarization of 75% was routinely achieved during previous experiments.

The target consists of a superconducting Helmholtz coils pair which operates at 5 Tesla, a ^{4}He evaporation refrigerator, a large pumping system, a high power microwave tube operating at frequencies around 140 GHz and an NMR system for measuring the target polarization. Figure 5 shows the target side view.

Figure 5: Sideview of the UVa polarized NH_3 target.

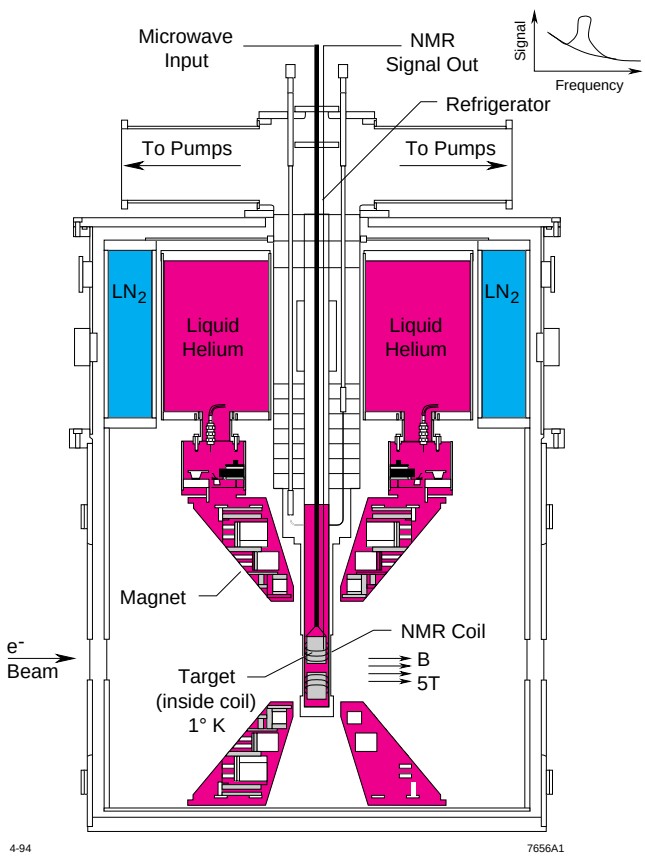

The target spin needs to be aligned at 139° w.r.t. the beamline. Figure 6 shows the orientation of the target field and coils. For safety reasons, about 5 mm clearance is required between the raster outer edge and the coils.

The target cell is filled with frozen ammonia granules (1-2 mm in size) which is fixed to a target holder stick (insert) and lowered into a cryostat of liquid ^{4}He. The nitrogen, helium and other target holder materials are in the acceptance of the spectrometers and will dilute the measured asymmetry. The thickness and density of each material are given in Table 1. The dilution factor will be discussed in Section 4.4. The packing factor is defined as the fraction of $^{15}NH_3$ to all materials in the target, and is usually measured using reference targets made of carbon disks (^{12}C) and ^{4}He. The unpaired proton in nitrogen can be polarized, hence a correction to the asymmetry must be made during analysis. The uncertainty due to the asymmetry from quasi-elastic scattering (QES) on nitrogen will be discussed in

Figure 6: Configuration of target coils.

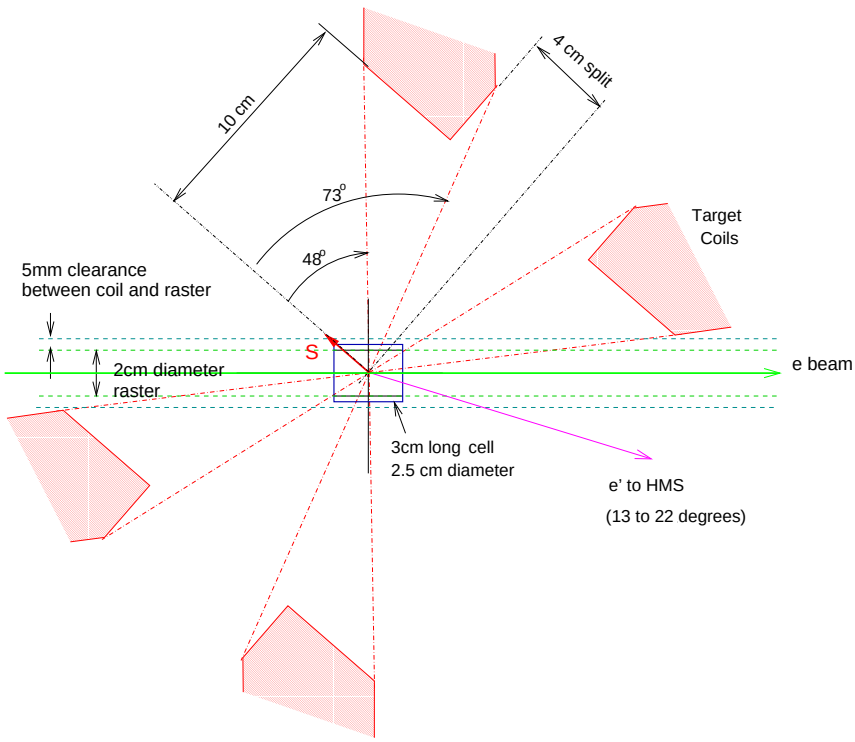

Section 4.5.

Table 1: Thickness and density for unpolarized materials along the beam-line.

Material	Thickness (cm)	Density (g/cm^3)
^{4}He (50% packing factor)	2.5	0.145
Al end-caps	0.00762	2.70
Copper in NMR coil	0.00673	8.96
Nickel in NMR coil	0.00289	8.75
Al windows in tail	0.00712	2.70
Al windows in LN_2 shield	0.00508	2.70
Al entrance window in cryostat†	0.00702	2.70
Al exit window in cryostat	0.01016	2.70

†the Al entrance window is not seen by the HMS, although it contributes to the radiation and energy loss before scattering.

The target polarization needed is 75% (average) with 85 nA beam, measured by NMR to $\Delta P_t/P_t = 2.5\%$. During previous experiments, the NMR measurement was done continuously during the run. NMR

readings were available every ≈ 20 seconds for on-line display, and were stored in special target event files for offline analysis. The price to pay for this is the presence of NMR pickup coils in the target cells, which should be accounted for in the dilution analysis. Figure 7 shows the geometry of the cell and the NMR coil used to measure proton polarization.

Figure 7: The 3 cm long by 2.5 cm diameter cylindrical target cell with the single loop coil used for measuring the proton polarization. Drawing not to scale.

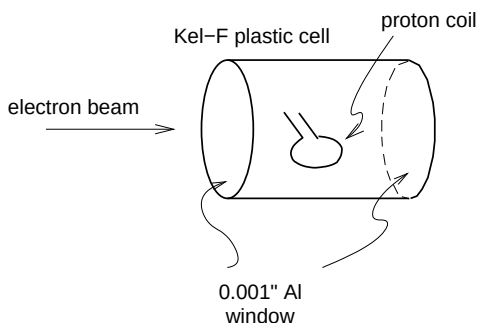

The radiation from the beam will lower the target polarization. This can be partially recovered by target annealing, a process where the $^{15}NH_3$ material is warmed from ≈ 1 K to ≈ 80 K. But eventually the target material needs to be changed for every 80 hours of 85 nA beam. We will use two cells per insert and at least one, probably two insert changes will be needed during the experiment. Each insert change takes approximately 20 hours. The first $4 \sim 6$ hours and the $6 \sim 8$ hours at the end of an insert change are for thermal equilibrium (TE) calibrations and should be performed with the hall closed. In order to minimize the uncertainty of target polarization, we plan to perform additional TE calibrations opportunistically during the experiment.

The strong magnetic field of the proposed target configuration will have an effect on the scattering charged particles but this can be well simulated. The uncertainty in the target spin direction is one of the main systematic uncertainties of this experiment. During previous experiments the field direction has been measured to 0.1°, and we require the same precision.

3.4 Spectrometer

For the proposed experiment, only scattered electrons will be detected. Elastic events are identified by the scattering angle and the momentum of electrons. Good angular and momentum resolutions will help to reduce the elastic peak width and the quasi-elastic background. We will use the High Momentum Spectrometer (HMS) for detecting scattered electrons. A shower counter (which is part of the standard equipment) is needed in HMS for rejecting pions. The central momentum of HMS can be calculated from the dipole field magnitude to a level of better than 1×10^{-3}. The central angle can be determined to 0.3 mrad. In Section 4.4, we will give the simulation results of both elastic and quasi-elastic events and estimate the dilution factor.

3.5 Acceptance Effect due to Target Magnetic Field

Due to the strong magnetic field the scattered electrons will be bent upward by $\approx 5^\circ$. This will cause a tilt of the scattering plane. The direct effects are that there is a correction to the target spin polar angle $\theta^\star$ and the azimuthal angle $\phi^\star \neq 0$. The corrected $\theta^\star$ and $\phi^\star$ will be given in Table 2. Figure 8 shows the HMS acceptance for electrons at $Q^2 = 0.61$ and 2.10 (GeV/c)^2. Overall, the bending is small and the scattering angle is close to the HMS central setting. The change in the counting rate is negligible.

Figure 8: HMS acceptance for $E' = 3.273$ (left) and 4.881 (right) electrons with (red) and without (black) target field. With target field electrons with initial $\phi_{targ} < 0$ (vertical up) will reach the center of HMS. Simulations were perfomed using SIMC with the HMS collimator IN in order to show clearly the shift in the acceptance.

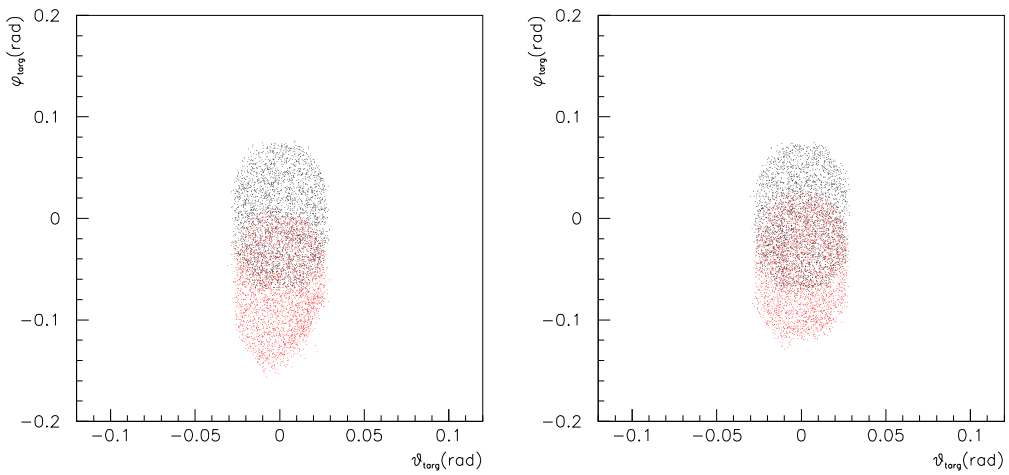

3.6 Low Q^2 Measurement

We will measure the elastic asymmetry at $Q^2 = 0.61$ (GeV/c)^2 with a statistical uncertainty of 2% to determine the absolute helicity state of the electron beam, and to check the product of target and beam polarizations. Since any change in the target spin orientation will bring addtional uncertainties to the target polarization, we will do the low Q^2 measurement with the same target spin direction as the high Q^2 running. For the same purposes, it is necessary to use a small scattering angle and a low beam energy such that the "theoretical" uncertainty due to the difference between Rosenbluth and polarization transfer data is small. However, due to limitation from the existing chicane system in Hall C, the lowest beam energy allowed for the proposed target field orientation is ≈ 3.3 GeV. Therefore we choose to use three pass beam. Due to a small out-of-plane component caused by the field bending of the scattered electrons, the scattering angle will be 13.45° with the HMS sitting at 13.10°. The total uncertainty of the measured asymmetry, besides that due to the beam and target polarizations, is 3.450%. The difference in the calculated asymmetry from the Bosted fit and polarization transfer fit is 5.33%. We take half of this value as the "theoretical uncertainty". Hence the low Q^2 measurement will provide a 4.4% check for the product of target and beam polarizations.

3.7 Data Analysis

The physics asymmetries can be extracted from the raw asymmetries as

$$A = \frac{A_{raw}(1-\eta_{A_{\rm N}})}{P_{beam}P_{targ}f} \tag{1}$$

where $P_{beam} = 80\%$ and $P_{targ} = 75\%$ are the beam and target polarizations, f is the target dilution factor and $\eta_{A_{\rm N}}$ is a correction factor due to the asymmetry of quasi-elastic scattering electrons from the nitrogen in $^{15}\mathrm{NH}_3$ (see Section 4.5 for the uncertainty of this correction).

The error in the asymmetry A is

$$\Delta A = \left\{\left(\frac{\Delta A_{raw}}{fP_bP_t}\right)^2 + A^2\left[(\frac{\Delta P_b}{P_b})^2 + (\frac{\Delta P_t}{P_t})^2 + (\frac{\Delta f}{f})^2\right]\right\}^{1/2}, \tag{2}$$

$$\text{with} \qquad \Delta A_{raw} = \frac{1}{\sqrt{N}}, \tag{3}$$

where N is total number of events. The ratio G_E^p/G_M^p is extracted using Eq. (16) and its uncertainty from Eq. (17) of Appendix A. Detailed formulas for the error propagation from other error sources are given in Appendices A and B.

4 Expected Uncertainties and Rate Estimation

In this section we first list all uncertainty sources. Then we calculate the rate, the expected total uncertainties on $\mu G_E^p/G_M^p$ and the beam time.

4.1 Experimental Systematics

We estimate the uncertainty in the beam polarization to be 1.5% and the target polarization has 2.5% uncertainty. Other error sources include those from the target spin angle, beam energy $\Delta E/E = 2\times10^{-4}$, HMS central momentum $\Delta E'/E' = 1\times10^{-3}$, and central angle $\Delta\theta = 0.3$ mrad [33]. Formula for error propagation from these experimental systematics to $\mu G_E^p/G_M^p$ are given in Appendix B. The largest systematic uncertainty comes from target polarization. At $\Delta P_{targ}/P_{targ} = 2.5\%$ the uncertainty in $\mu G_E^p/G_M^p$ is about $2/3$ of the statistical uncertainty.

4.2 Beam Charge Asymmetry

The beam charge is measured by the beam current monitor (BCM). The overall uncertainty in the BCM is about 5%. However the uncertainty in the beam charge asymmetry is expected to be much smaller than this value. In Ref. [36], the uncertainty on the beam charge asymmetry comes from (1) 1% from calibration offset; (2) 50 ppm from noise in the BCM signal; (3) 0.5% from the stability of the offset; and (4) ≈ 10 ppm from non-linearity for 85 nA current. The uncertainty on $\mu G_E^p/G_M^p$ due to beam charge asymmetry is about half of the error due to the target polarization (the latter is the dominant term of systematic uncertainties).

4.3 Target Polarization

Target polarization can be measured to 2.5% using NMR, as mentioned in Section 3.3. To minimize the uncertainty on the target polarization, we will perform additional thermal equilibrium (TE) calibration(s)

opportunistically during the experiment, *i.e.* everytime when the beam is expected to be down for more than 6 hours. TE calibration should be performed with the hall closed.

4.4 Target Dilution Factor

The dilution factor is due to the quasi-elastic events from nitrogen in NH_3 and from other material listed in Table 1. Since the reconstructed elastic peak at forward angles typically has a FWHM less than 20 MeV, while quasi-elastic events are smeared by Fermi motion, about 80% of quasi-elastic events will be excluded using a cut in $\delta E' \equiv E' - E'_{el}$ where E'_{el} is the electron energy measured by HMS and E'_{el} is the energy of elastically scattered electrons calculated from the scattering angle θ. Figure 9 shows the simulated elastic events (red), quasi-elastic events (green) and the sum (blue) for 1 mC beam charge.

Figure 9: Expected spectra on $\delta E' \equiv E' - E'_{el}$ for the proposed measurements at $Q^2 = 0.61$ (top), 2.10 (middle) and 3.50 (GeV/c)^2 (bottom). Simulations were performed using SIMC without HMS collimators, ^{15}N and ^{4}He quasi-elastic events were simulated using the ^{12}C spectral function in the independent particle shell model (IPSM) and all other material were using the ^{56}Fe IPSM spectral function. The blue shows the sum of elastic and quasi-elastic events. Black lines show cut in $\delta E'$ used to obtain elastic rate and dilution f.

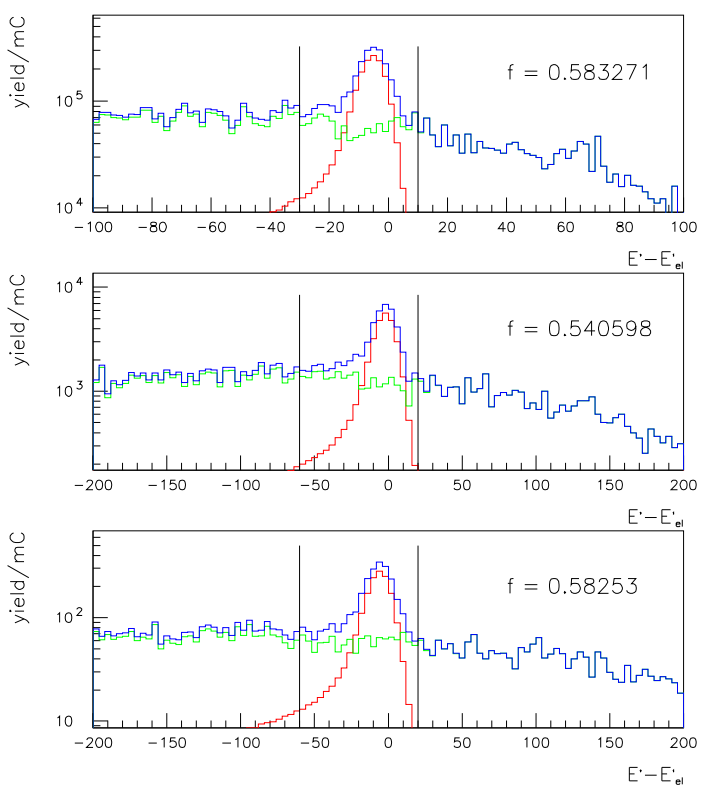

The dilution factor is defined as

$$f = \frac{N_p}{N_p + N_{\mathrm{QE}}} \tag{4}$$

where N_p and N_{QE} are, respectively, yield of $e-p$ elastic events and quasi-elastic events from ^{15}N and other target material. Since the actual angular resolution of the HMS is usually not as good as the COSY model used in the simulation, we use $f = 0.5$ as a conservative estimate for all three kinematics in the rate and uncertainty estimation. This value is also consistent with a previous experiment [37].

We will take data on carbon disks and He with approximately the same geometry as the NH_3 cell to measure the quasi-elastic cross sections, from which the dilution factor can be calculated. In E01-006 [37], the dilution factor is expected to be determined to an accuracy of $(2.5-3)\%$ over the final state invariant mass range $0.8 \leqslant W \leqslant 2$ GeV. We expect to achieve a 2.5% uncertainty at the elastic peak.

4.5 Nitrogen Asymmetry

The nitrogen in $^{15}NH_3$ is polarized and will contribute to the asymmetry. In the shell model, the ^{15}N nucleus has one unpaired proton which can be polarized. The polarization of the unpaired proton in ^{15}N is reduced from that of a free proton by several factors. First, the nitrogen in ^{15}N is polarized up to only $1/6$ of the proton, based on the Equal Spin Temperature (EST) hypothesis. Fig. 10 shows data from Paul Scherrer Institute (PSI) in Switzerland and from SLAC experiments E143 and E155x, compared with EST predictions. Secondly, the proton in a polarized ^{15}N is only polarized to a certain amount.

Figure 10: Polarization of nitrogen P_N in $^{15}NH_3$ *vs.* proton polarization P_p measured at PSI and during SLAC experiments E143 and E155x. The solid curve represents the prediction in the Equal Spin Temperature (EST) hypothesis and the dashed curve is a fit to world data.

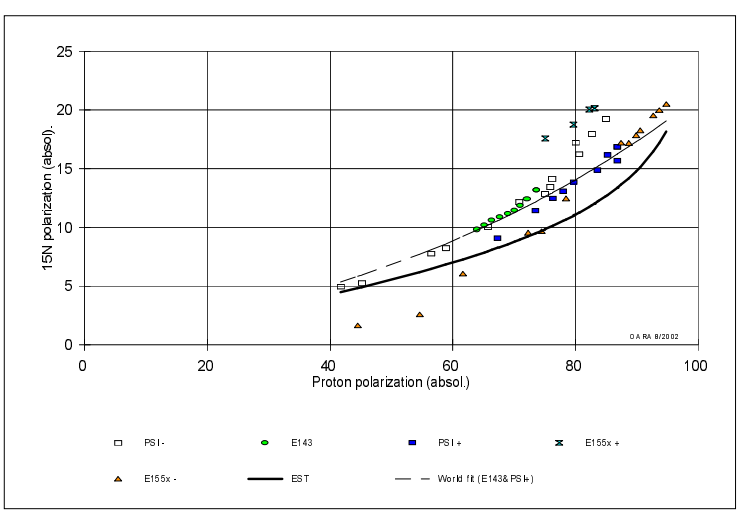

This quantity, called the effective nucleon polarization, has been estimated in two ways. In a model independent method [41, 42], $P_{p/^{15}\mathrm{N}} \approx -0.22$ based on isospin symmetry and data from beta decay of the mirror nucleus ^{15}O. In the shell model, the proton in ^{15}N is aligned anti-parallel to the nuclear

spin $1/3$ of the time, hence $P_{p/^{15}\mathrm{N}} = -0.33$. Overall, the polarization of the unpaired proton is at most $(0.22 \sim 0.33) \times 1/6 P_p = 0.037 \sim 0.055 P_p$. In addition, only about $1/15$ of ^{15}N quasi-elastic (QE) events are from the $p_{1/2}$ proton, and not all the QE events are from the ^{15}N. The fraction of ^{15}N to total QE events is about $2/3$, which can be calculated from the packing factor measured using carbon disks and ^{4}He as in E01-006 [37]. Also, there are three protons in $^{15}\mathrm{NH}_3$. The correction to the measured asymmetry A_m due to nitrogen is therefore

$$A_m = f A_p + \frac{1}{3}\frac{2}{3}\frac{(1-f)}{15} A_{p/^{15}\mathrm{N}} = f A_p \Big(1 + (0.00054 \sim 0.00082)\frac{1-f}{f}\Big) \quad (5)$$

$$A_p = \frac{A_m}{f}\Big(1 - (0.00069 \pm 0.00014)\Big) \quad \text{if } f = 0.5 \quad (6)$$

Compared to the usually used $A = \frac{A_m}{f}$, we need to apply a 0.069% correction with $\pm 0.014\%$ uncertainty for all three Q^2 points.

4.6 Background

For our measurement the main background comes from the quasi-elastic scattering from nitrogen and materials on the beam path. This part was discussed in the last section. The π^- background was estimated using Lightbody's code [43] and is found to be negligible. In addition, π^-'s will be rejected by the shower counter, which has a pion rejection factor of $\approx 100:1$. Therefore we expect no effect from the pions on the measured asymmetry.

4.7 Electromagnetic Radiative Corrections

We discuss here electromagnetic radiative corrections besides possible large corrections from the two-photon exchange process. The "traditional" radiative corrections can be calculated using Mo and Tsai's formalism [21] and the uncertainty of the correction to elastic asymmetries is negligible.

4.8 Deadtime Correction

The total rate of our proposed measurement is very low, a few tens of Hz, hence the electronic dead time correction is small and the effect on the measured asymmetry is negligible. Computer deadtime can be measured by triggers and the uncertainty is determined by the statistics of each run. We require a run to have at least 1M events hence the uncertainty in the measured deadtime is 0.1%.

4.9 Optimization of Kinematics

We optimize the kinematics based on the following conditions:

- For a given Q^2, the rate is maximized by varying beam energy and scattering angle;
- For given Q^2 and beam energy, the total uncertainty of $\mu G_E^p/G_M^p$ is minimized by varing target spin angle;
- Target coils do not interfere with either beam-line or scattered electrons. A 0.5 cm clearance is required between coils and outer edge of particle trajectory.

Figure 11: Expected total uncertainties of $\mu G_E^p/G_M^p$ *vs.* target spin angle for $E = 6$ GeV and fixed beam time, 46.1 and 245.5 hours for $Q^2 = 2.10$ and 3.50 (GeV/c)^2, respectively. Here negative spin angle means the target spin is pointing to the left of beam-line. Red (blue) boxes show the interference between coils and beam-line (scattered electrons). Red stars show the selected kinematics.

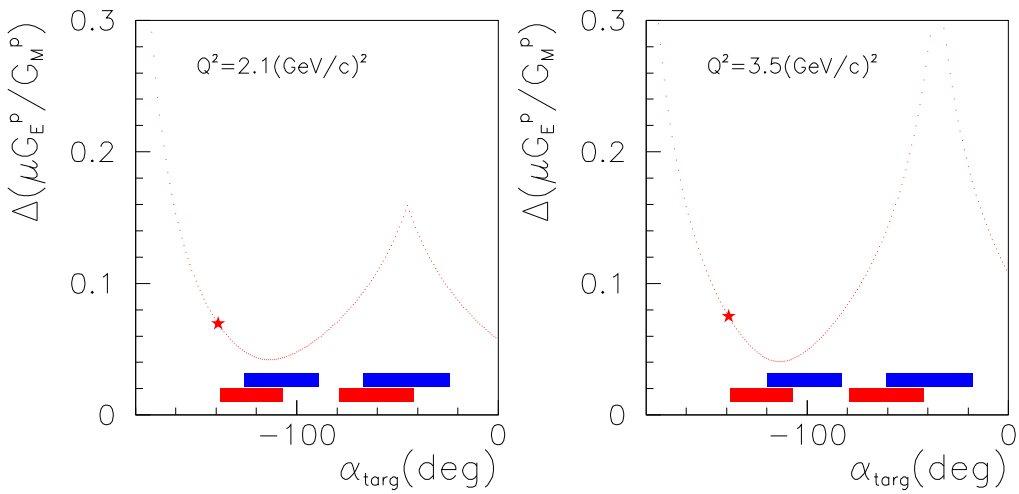

Figure 12: Expected total uncertainties of $\mu G_E^p/G_M^p$ *vs.* beam energy for fixed beam time, 46.1 and 245.5 hours for $Q^2 = 2.10$ and 3.50 (GeV/c)^2, respectively. Hence we choose to use a 6 GeV beam.

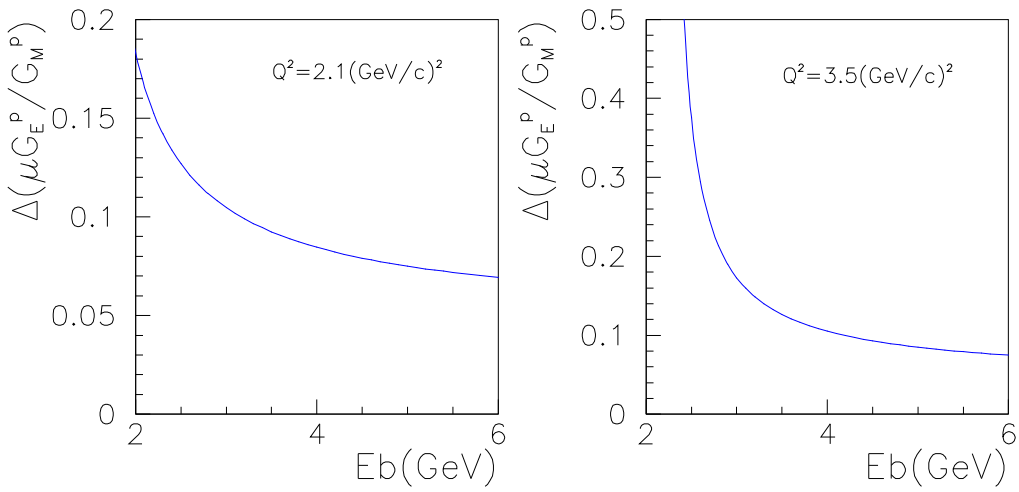

Results are shown in Fig. 11 and 12. We choose to use a 6 GeV beam. Target spin will be pointing to the left and aligned at 139° *w.r.t* the beam-line.

4.10 Summary of Rate and Expected Uncertainties

We use the Bosted fit for G_M^p and G_E^p to calculate the elastic $e-p$ cross section. Using a 3 cm target cell and 85 nA beam current the luminosity available is 8.5×10^{34} cm^2/s. The expected results are shown in Fig. 13. Kinematics, rates and expected uncertainties for the proposed measurements are given in Table 2, where

◇ E is beam energy;
◇ θ_e and E' are the energy and momentum of scattered electrons (HMS);
◇ θ_p and p_p are the energy and momentum of scattered protons (not detected);
◇ $\theta^\star$ and $\phi^\star$ are the polar and azimuthal angles of target spin;
◇ A_{el} and $A_{el,bosted}$ are elastic asymmetries calculated from Hall A polarization transfer (PT) fit and Bosted fit, respectively;
◇ A_{raw} is expected measured asymmetry using PT fit;
◇ N_{tot} is total number of events in elastic peak;
◇ Systematic uncertainty on asymmetries including 1.5% from beam polarization, 2.5% from target polarization, 2.5% from target dilution factor, $\approx 1.2\%$ from charge asymmetry, 0.35% from QE events from nitrogen, and 0.1% from deadtime correction.

Figure 13: Expected results and full uncertainties of the proposed measurements (red solid circles) along with world data. Curves are from the Bosted parameterization (solid) [16], a fit to the Hall A polarization transfer results (dashed) [13] and a global fit to the cross section data (dash-dotted) [17].

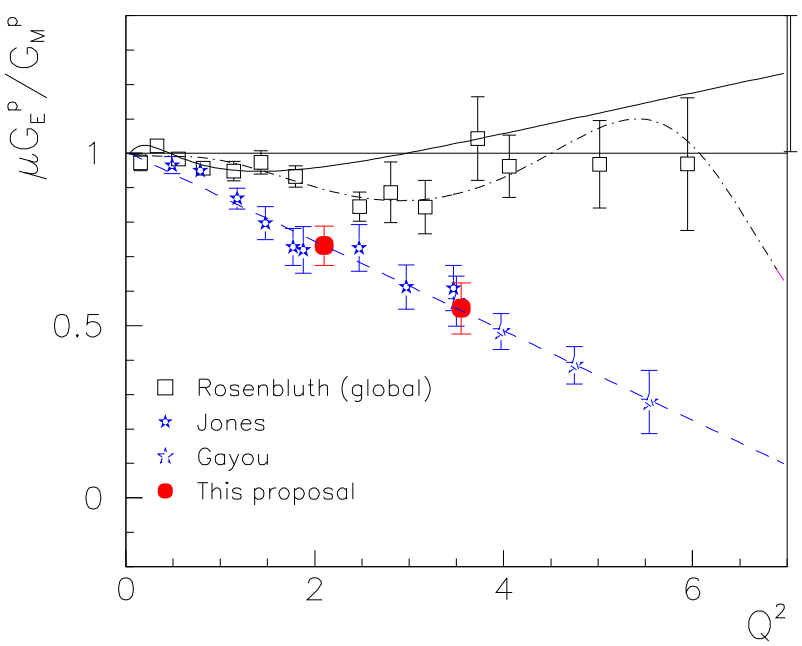

Table 2: Kinematics, rate and expected uncertainties for the proposed measurements.

Q^2 (GeV/c)^2	0.61	2.10	3.50
E (GeV)	3.60	6.00	6.00
θ_e	13.45°	15.39°	21.65°
E' (GeV)	3.273	4.881	4.135
θ_p	60.95°	45.03°	35.27°
p_p (GeV/c)	0.849	1.831	2.642
$\theta^\star$	78.03°	93.98°	103.75°
$\phi^\star$	177.98°	178.51°	177.89°
A_{el}	0.078	0.119	0.200
A_{raw}	0.0234	0.0357	0.0599
$(A_{el,bosted} - A_{el})/A_{el}$	5.33%	17.56%	27.60%
σ (nb/sr)	375.215	5.893	0.332
elastic rate (SIMC, Hz)	141.430	2.600	0.148
total rate (el rate/f, Hz)	282.860	5.200	0.296
N_{tot}	4572K	862K	262K
Uncertainty on asymmetries			
Statistical	2.000%	3.016%	3.265%
Systematic	2.811%†	4.050%	4.050%
Total	3.450%†	5.050%	5.202%
Uncertainty on $\mu G_E^p/G_M^p$			
$\Delta P_{beam}/P_{beam} = 1.5\%$	-	0.0174	0.0222
$\Delta P_{targ}/P_{targ} = 2.5\%$	-	0.0290	0.0370
Target dilution $\Delta f/f = 2.5\%$	-	0.0290	0.0370
Beam charge asymmetry	-	0.0146	0.0178
Nitrogen asymmetry	-	0.0006	0.0007
Deadtime correction	-	0.0012	0.0015
$\Delta E/E = 5 \times 10^{-4}$	-	0.0001	0.0001
$\Delta E'/E' = 1 \times 10^{-3}$	-	0.0008	0.0005
$\Delta\theta_e = 0.3$ mrad	-	0.0002	0.0001
Target spin orientation (inp) 0.1°	-	0.0097	0.0069
Target spin orientation (oop) 0.1°	-	0.0024	0.0025
Total syst.	-	0.0480	0.0600
Total stat.	-	0.0350	0.0483
Beam time (hours)	4.5	46.1	245.5
Expected $\mu G_E^p/G_M^p$ and total uncertainty	-	0.732 ± 0.057	0.550 ± 0.074

† since the low Q^2 measurement is to check the product of beam and target polarizations $P_b P_t$, we do not include the uncertainties due to P_b and P_t here;

5 Beam Time Request

Our beam time request is given in Table 3. We ask for 14 PAC days for production data taking, target dilution factor measurement, Møller and arc measurements. We ask for 3 PAC days overhead time for one beam pass change and target work. If this experiment can run together with the approved E03-109 [45], then no additional time for target installation will be needed.

Table 3: Spectrometer settings, total beam time and overhead time for the proposed measurements.

Q^2 (GeV/c)^2	0.61	2.10	3.50
E (GeV)	3.60	6.00	6.00
θ_{HMS}	13.10°	15.39°	21.65°
p_{HMS} (GeV/c)	3.273	4.881	4.135
Production time	4.5	46.1	245.5
carbon and helium runs	2	4	12
Møller measurement	1	2	9
arc measurement	4	4	
Total beam time (PAC hours)		334	
One pass change		8	
HMS configuration change		6	
Target field survey		10	
Target anneal		56	
Two target insert changes		40	
Total overhead (clock hours)		120	

6 Comparison to Other Methods

In this section we compare the proposed measurements with other elastic scattering asymmetry methods.

6.1 Comparison to Coincidence and Single-Proton Measurement

One of the main systematic uncertainties of the proposed measurements comes from the target dilution factor. One possible solution is to perform coincidence measurement, using the HMS for protons and a calorimeter for electrons. In this case, most of the quasi-elastic events from the nitrogen are excluded in the phase space. From simulation we obtain a dilution factor $f > 0.9$, with a possibly smaller uncertainty of $\Delta f/f \approx 1\%$ than the single arm measurement. However, the main problem of a coincidence measurement is how to choose the kinematics (target spin orientation and beam energy) such that both scattered protons and electrons are not blocked by the target coils, while keeping a good sensitivity to G_E^p/G_M^p. We compared coincidence vs. single electron measurements taking into account (1) the constraints from the target coils; (2) dilution factor $f \approx 0.9$ for coincidence and $f \approx 0.5$ for single arm measurement; and (3) different error propagation from the asymmetry to G_E^p/G_M^p, and found that in order to achieve the same total uncertainty on G_E^p/G_M^p, we need $\approx 20\%$ more beam time for coincidence measurement. Also, the main advantage of single arm over coincidence is that it has a very simple set up, which has been used before three times in Hall C – all subsystems involved in this proposal are available and have been used before.

We also compared single-arm electron with single-arm proton measurements. The advantage of single-arm proton measurement is a smaller dilution effect from the nitrogen since only quasi-elastic events from the protons inside the nitrogen are counted by the HMS. However, for the proposed kinematics, the ratio of proton to electron rate for fixed solid angle accptance is about $3:4$ and the gain in the dilution factor does not compensate the loss in the counting rate.

6.2 Comparison to PR01-105

In principle, G_E/G_M is directly related to the ratio of transverse ($\theta^\star = 90$) and longitudinal ($\theta^\star = 0$) asymmetries A_T/A_L, as can be seen from Eq. (12). Also it has the advantage that uncertainties due to beam and target polarizations and target dilution factor drop out when taking the ratio, hence largely reduce the systematic uncertainty on G_E^p/G_M^p. This method was proposed [47] to PAC-20, of which the authors asked for 330 hours of total beam time to measure G_E^p/G_M^p at $Q^2 = 1.1$ and 2.1 (GeV/c)^2 with good precision. First, we would like to point out that the Q^2 value of PR01-005 is low, where the discrepancy between the Rosenbluth and the polarization transfer data sets is not as significant as this proposal. Secondly, to make a comparison between the A_T/A_L method and this proposal, let's look at the $Q^2 = 3.50$ (GeV/c)^2 point. To achieve the same uncertainty on $\mu G_E^p/G_M^p$, one needs to measure ratio A_T/A_L to the same level as the total uncertainty on the proposed asymmetry A_{pr}, *i.e.* a statistical error of $\Delta(A_T/A_L)/(A_T/A_L) = 4.97\%$, assuming zero systematic uncertainty. At this kinematics $A_T = 0.045$ and $A_L = -0.236$, the uncertainty $\Delta(A_T/A_L)$ is approximately ΔA_T magnified by factor $1/A_L \approx 4.2$. Hence one needs to measure A_T to a level of $\Delta A_T/A_T = 1.2\%$. We can estimate the beam time by comparing this value to the statistical error on the asymmetry ($\Delta A_{pr}/A_{pr} = 3.2\%$) proposed here, the beam time required will be ≈ 7.1 times longer. Therefore we believe the proposed method is better than PR01-105. Note that we optimize the kinematic setting for the $Q^2 = 3.50$ (GeV/c)^2 point, hence one should not directly compare the $Q^2 = 2.10$ (GeV/c)^2 measurement of this proposal with that of PR01-105.

The PAC-20 report on PR01-105 is given in Appendix C. The main reason that PR01-105 was deferred was because of an approved precision Rosenbluth experiment [18], which was expected to check the discrepancy between data from the Rosenbluth separation and the polarization transfer method. Now this experiment has been completed and their preliminary results agree well with traditional Rosebluth data and thus the discrepancy is not resolved. On the other hand, theoretical effort on understanding this discrepancy is not mature enough to give a good explanation. Hence we believe this is the right time to provide another check from a new method, to fully understand the proton form factor data.

7 Summary

We propose to make measurements of G_E^p/G_M^p via the asymmetry in doubly polarized elastic $\vec{p}(\vec{e},e')p$ scattering at $Q^2 = 2.10$ and 3.50 (GeV/c)^2. Assuming 80% beam polarization and 85 nA current, we request 14 days of beam time and 3 days overhead. The proposed measurement will provide the first data for G_E^p/G_M^p from the $\vec{p}(\vec{e},e')p$ asymmetry method in intermediate Q^2 range, with good precision. This new method is expected to be less sensitive to two-photon exchange contributions than the Rosenbluth separation technique, and it does not suffer from the same systematic uncertainties as previous polarization transfer measurements. These data will provide an important check on the polarization transfer results. When combined with the recent check on the Rosenbluth separation results, the new data will either confirm that two-photon exchange or other missing physics is a necessary ingredient in future calculations, or they will point to a possible systematic error in prior experimental techniques.

A Doubly Polarized Elastic Scattering

For elastic scattering the unpolarized cross section is given by

$$\left(\frac{\mathrm{d}^2\sigma}{\mathrm{d}\Omega\mathrm{d}E'}\right)^u = \sigma_M \frac{E'}{E}\left(\frac{G_E^2+\tau G_M^2}{1+\tau} + 2\tau G_M^2 \tan^2(\theta/2)\right), \tag{7}$$

where $Q^2 = 4EE'\sin^2(\theta/2)$, $\tau = Q^2/(4M^2)$, the energy of scattered electrons is $E' = E/\left[1+\frac{2E}{M}\sin^2(\theta/2)\right]$, M is the nucleon mass, E is the beam energy and θ is the electron scattering angle. The Mott cross section is

$$\sigma_M \equiv \left(\frac{\mathrm{d}\sigma}{\mathrm{d}\Omega}\right)_{Mott} = \frac{\alpha^2\cos^2\frac{\theta}{2}}{4E^2\sin^4\frac{\theta}{2}}. \tag{8}$$

The momentum and the angle of the scattered protons are

$$p_p = \sqrt{Q^2 + (\frac{Q^2}{2M})^2} \text{ and} \tag{9}$$

$$\cos\theta_p = \frac{(M+E)\sqrt{M^2+p_p^2} - M^2 - ME}{p_p E}. \tag{10}$$

For the case of polarized electrons scattering off a polarized nucleon target, the cross section difference between opposite electron helicity states is given by [46]

$$\frac{1}{2}\left[\sigma^+ - \sigma^-\right] = -2\sigma_M \frac{E'}{E}\sqrt{\frac{\tau}{1+\tau}}\tan\frac{\theta}{2}\left\{\sqrt{\tau\left(1+(1+\tau)\tan^2\frac{\theta}{2}\right)}\cos\theta^\star G_M^2 + \sin\theta^\star\cos\phi^\star G_M G_E\right\}, \tag{11}$$

where the superscript $\pm$ denotes the helicity of the incident electrons, θ^* and ϕ^* are the polar and the azimuthal angles of the target spin direction as shown in Fig. 14. The asymmetry is

$$\begin{aligned} A &\equiv \frac{\sigma^+ - \sigma^-}{\sigma^+ + \sigma^-} \\ &= -\frac{2\sqrt{\frac{\tau}{1+\tau}}\tan\frac{\theta}{2}\left\{\sqrt{\tau\left(1+(1+\tau)\tan^2\frac{\theta}{2}\right)}\cos\theta^\star G_M^2 + \sin\theta^\star\cos\phi^\star G_M G_E\right\}}{\frac{G_E^2+\tau G_M^2}{1+\tau} + 2\tau G_M^2\tan^2(\theta/2)}, \end{aligned} \tag{12}$$

Equation (12) can be written as

$$(\frac{G_E}{G_M})^2 + B(\frac{G_E}{G_M}) + C = 0, \tag{13}$$

where

$$B = \frac{2}{A}\sqrt{\tau(1+\tau)}\tan\frac{\theta}{2}\sin\theta^\star\cos\phi^\star, \tag{14}$$

$$C = \tau + 2\tau(1+\tau)\tan^2\frac{\theta}{2} + \frac{2\cos\theta^\star}{A}\left\{\sqrt{\tau(1+\tau)}\tan\frac{\theta}{2}\sqrt{\tau\left[1+(1+\tau)\tan^2\frac{\theta}{2}\right]}\right\} \tag{15}$$

Figure 14: Polar and azimuthal angles of the target spin. Here $\vec{S}$ is the target spin, $\vec{q}$ is the three momentum transfer. The $z^\star$ axis is defined by $\vec{q}$, $y^\star$ axis is defined by $\vec{k} \times \vec{k}'$ with $k(k')$ the three momentum of the incident and scattered electrons.

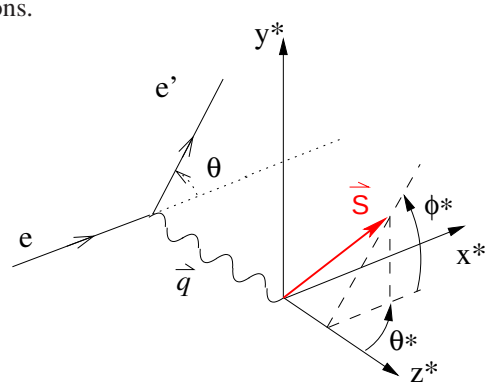

with A the measured elastic asymmetry. Therefore ratio G_E/G_M can be calculated as

$$\frac{G_E}{G_M} = \frac{1}{2}\left(-B \pm \sqrt{B^2-4C}\right), \tag{16}$$

the sign is kinematic dependent. The uncertainty due to the error in asymmetry is given by

$$\Delta\left(\frac{G_E}{G_M}\right) = \frac{\Delta A}{2}\left|\left(\frac{\mathrm{d}B}{\mathrm{d}A}\right)\left(-1 \pm \frac{B}{\sqrt{B^2-4C}}\right) \pm \left(\frac{\mathrm{d}C}{\mathrm{d}A}\right)\frac{-2}{\sqrt{B^2-4C}}\right| \tag{17}$$

$$\text{where} \quad \frac{\mathrm{d}B}{\mathrm{d}A} = -\frac{B}{A}$$

$$\text{and} \quad \frac{\mathrm{d}C}{\mathrm{d}A} = -\frac{C-\left[\tau+2\tau(1+\tau)\tan^2\frac{\theta}{2}\right]}{A}$$

B Error Propogation of Systematic Uncertainties for G_E^p/G_M^p

The uncertainty in G_E^p/G_M^p due to the uncertainty in asymmetry ΔA is given by Eq. (17) where ΔA is from Eq. (2). In this appendix we give experimental systematics due to uncertainties in E, E', θ, $\theta^\star$ and $\phi^\star$.

From Eq. (16) the uncertainty in G_E/G_M due to the uncertainty in E is given by

$$\Delta\left(\frac{G_E}{G_M}\right) = \frac{\Delta E}{2}\left|\left(\frac{\mathrm{d}B}{\mathrm{d}E}\right)\left(-1 \pm \frac{B}{\sqrt{B^2-4C}}\right) \pm \left(\frac{\mathrm{d}C}{\mathrm{d}E}\right)\frac{-2}{\sqrt{B^2-4C}}\right| \tag{18}$$

the same equation stands for E', θ, $\theta^\star$ and $\phi^\star$. For E we have

$$\frac{\mathrm{d}B}{\mathrm{d}E} = \frac{\partial B}{\partial \tau}\frac{\mathrm{d}\tau}{\mathrm{d}E}, \quad \frac{\mathrm{d}C}{\mathrm{d}E} = \frac{\partial C}{\partial \tau}\frac{\mathrm{d}\tau}{\mathrm{d}E} \tag{19}$$

where

$$\frac{\partial B}{\partial \tau} = \frac{1}{2}\left(\frac{B}{\tau} + \frac{B}{1+\tau}\right),$$

$$
\begin{aligned}
\frac{\partial C}{\partial \tau} &= 1 + 2(1+\tau)\tan^2\frac{\theta}{2} + \frac{\tan\frac{\theta}{2}}{2A}\cos\theta^\star\left\{2\sqrt{(1+\tau)\left[1+(1+\tau)\tan^2\frac{\theta}{2}\right]}\right. \\
&\quad \left. + \sqrt{\frac{1+(1+\tau)\tan^2\frac{\theta}{2}}{1+\tau}} + \tau\tan\frac{\theta}{2}\sqrt{\frac{1+\tau}{1+(1+\tau)\tan^2\frac{\theta}{2}}}\right\} \\
\text{and } \frac{\mathrm{d}\tau}{\mathrm{d}E} &= \frac{\tau}{E}\,, \qquad (20)
\end{aligned}
$$

For θ we have

$$
\frac{\mathrm{d}B}{\mathrm{d}\theta} = \frac{\mathrm{d}B}{\mathrm{d}\theta} + \frac{\partial B}{\partial \tau}\frac{\mathrm{d}\tau}{\mathrm{d}\theta}\,, \quad \frac{\mathrm{d}C}{\mathrm{d}\theta} = \frac{\mathrm{d}C}{\mathrm{d}\theta} + \frac{\partial C}{\partial \tau}\frac{\mathrm{d}\tau}{\mathrm{d}\theta} \qquad (21)
$$

where

$$
\frac{\mathrm{d}\tau}{\mathrm{d}\theta} = \frac{EE'}{2M^2}\sin\theta\,, \quad \frac{\mathrm{d}B}{\mathrm{d}\theta} = \frac{B}{\sin\theta}
$$

For E' we have

$$
\frac{\mathrm{d}B}{\mathrm{d}E'} = \frac{\partial B}{\partial \tau}\frac{\mathrm{d}\tau}{\mathrm{d}E'} + \frac{\mathrm{d}B}{\mathrm{d}\theta^\star}\frac{\mathrm{d}\theta^\star}{\mathrm{d}E'}\,, \quad \frac{\mathrm{d}C}{\mathrm{d}E'} = \frac{\partial C}{\partial \tau}\frac{\mathrm{d}\tau}{\mathrm{d}E'} + \frac{\mathrm{d}C}{\mathrm{d}\theta^\star}\frac{\mathrm{d}\theta^\star}{\mathrm{d}E'} \qquad (22)
$$

$$
\text{where } \frac{\mathrm{d}\tau}{\mathrm{d}E'} = \frac{\tau}{E'}\,.
$$

The target spin polar angle $\theta^\star$ is determined by the field orientation and the proton scattering angle. The target field direction can be measured to 0.1° and the uncertainty in the proton angle is determined by the electron momentum $\Delta E'/E'$ as

$$
\frac{\mathrm{d}\theta^\star}{\mathrm{d}E'} = \frac{\mathrm{d}\theta_p}{\mathrm{d}E'} = \frac{(M+E)M}{\left(2M+\nu\right)^{3/2}E\sin\theta_p}\,. \qquad (23)
$$

C PAC-20 report for PR01-105

Individual Proposal Report

Proposal: PR-01-105

Title: G_{Ep} / G_{Mp} via Simultaneous Asymmetry Measurements of the Reaction $\vec{p}(\vec{e},e')$

Spokesperson: G. Warren

Motivation: The ratio G_{Ep} / G_{Mp} is vital to our understanding of the structure of the proton. Results from Hall A experiments using electron-proton polarization transfer have shown that this ratio clearly decreases with increasing Q^2. An experiment based on the Rosenbluth separation method (E-01-001) has been approved to check on these findings. The proposed experiment aims at providing another check with different systematic uncertainties and high statistical precision.

Measurement and Feasibility: The polarized beam polarized target asymmetry is to be measured simultaneously, using two spectrometers at the same Q^2, for different orientations of the proton polarization. The ratio of both cross sections is a function of G_{Ep} / G_{Mp} . In this ratio the degrees of polarization and the dilution factor of the target drop out to first order, thus minimizing systematic uncertainties. It is proposed to measure G_{Ep} / G_{Mp} at Q^2=1.1 and 2.1 $(GeV/c)^2$.

Issues: The proposal is clearly written and the underlying idea is very good. However, given the existing data and the approved experiment to check on them, the PAC does not find a compelling reason to approve this proposal at the present time.

Recommendation: Defer

Scientific Rating: N/A

References

[1] F. Iachello, A.D. Jackson, A. Lande, *Phys.Lett.B* **43**, 191 (1973); E.L. Lomon, *Phys. Rev. C* **64**, 035204 (2001).

[2] S.J. Brodsky and G. Farrar, *Phys. Rev. D* **11**, 1309 (1975).

[3] S.J. Brodsky and G.P. Lepage, *Phys. Rev. D* **22**, 2157 (1981).

[4] P.L. Chung and F. Coester, *Phys. Rev. D* **44**, 229 (1991).

[5] M.R. Frank, B.K. Jennings and G.A. Miller, *Phys. Rev. C* **54**, 920 (1996).

[6] R.F. Wagenbrunn *et al.*, *Phys. Lett. B* **511**, 33 (2001); S. Boffi *et al. Eur. Phys. J. A* **14**, 17 (2002).

[7] F. Cardarelli and S. Simula, *Phys. Rev. C* **62**, 065201 (2000); S. Simula, e-Print nucl-th/0105024.

[8] D.H. Lu, A.W. Thomas and A.G. Williams, *Phys. Rev. C* **57**, 2628 (1998).

[9] G.Holzwarth, *Zeitschr. Fuer Physik A* **356**, 339 (1996), e-Print hep-ph/9606336; e-Print hep-ph/0201138 and ref. therein.

[10] A.F. Sill *et al.*, *Phys. Rev. D* **48**, 29 (1993).

[11] J. Arrington, e-Print nucl-ex/0309011.

[12] M.K. Jones *et al.*, *Phys. Rev. Lett.* **84**, 1398 (2000).

[13] O. Gayou *et al.*, *Phys. Rev. Lett.*, **88**, 092301 (2002).

[14] O. Gayou *et al.*, *Phys. Rev. C* **64**, 038202 (2003).

[15] J. Arrington, *Eur. Phys. J.* **A17**, 311 (2003); *Phys. Rev.C* **68**, 034325 (2003).

[16] P. Bosted, *Phys. Rev. C* **51**, 409 (1995).

[17] H. Budd, A. Bodek and J. Arrington, *to be published in Nucl. Phys. B*, e-Print Archive: hep-ex/0308005.

[18] J. Arrington and R. Segel, JLab E01-001, New Measurement of (GE/GM) for the Proton.

[19] E. Brash, C. Perdrisat and V. Punjabi, JLab E01-109, Measurement of Gep/Gmp to Q2=9 GeV2 via Recoil Polarization.

[20] J. Mar *el al. Phys. Rev. Lett.* **21**, 482 (1968).

[21] L. Mo, Y.S. Tsai, *Rev. Mod. Phys.* **41**, 205 (1969).

[22] P.A.M. Guichon and M. Vanderhaeghen, e-Print: hep-ph/0306007.

[23] P.G. Blunden, W. Melnitchouk and J.A. Tjon, e-Print: nucl-th/0306076.

[24] M.P. Rekalo and E. Tomasi-Gustafsson, e-Print: nucl-th/0307066.

[25] E.J. Brash, *et al.*, e-Print: hep-ex/0111038.

[26] J. Arrington, e-Print: nucl-ex/0311019.

[27] A. Afanasev, *priv. comm.*

[28] A. De Rujula, J.M. Kaplan, and E. De Rafael, *Nucl. Phys.* **B53**, 545 (1973).

[29] A. Afanasev, I. Akushevich, and N.P. Merenkov, e-Print: hep-ph/0208260.

[30] T. Powell, *et al. Phys. Rev. Lett.* **24**, 753 (1970).

[31] X. Jiang, private communication. X. Jiang and A. Afanasev, LAST LOI, 2003.

[32] S.P. Wells, *et al.*, *Phys. Rev. C.* **63**, 064001 (2001).

[33] Uncertainties on the beam-line instrumentation and the HMS, if not explicitly specified, are values that were routinely achieved in Hall C.

[34] H.-G. Zhu, *Ph.D. thesis*, Univ. of Virginia, Charlottesville, VA (2000).

[35] D. Day, JLab E93-026, The Charge Form Factor of the Neutron.

[36] G. Warren, O. Rondon, F. Wesselmann and M. Zeier, *Uncertainties in the Beam Charge Asymmetry for Gen01*, report to the E93-026 collaboration, (Sept.20, 2002).

[37] O. Rondon-Aramayo, JLab E01-006, Precision Measurement of the Nucleon Spin Structure Functions in the Region of the Nucleon Resonances.

[38] M. Steinacher, I. Sick, *Nucl. Instrum. Method A* **455**, 759 (2000).

[39] P.E. Raines, *Ph.D. thesis*, Univ. of Pennsylvania, (1996).

[40] H.-G. Zhu, *priv. comm.*

[41] K. Sugimoto, *Phys. Rev.* **182**, 1051 (1969).

[42] O.A. Rondon, *Phys. Rev. C* **60**, 035201 (1999).

[43] J.W. Lightbody, Jr., J.S. O'Connell, *Computers in Physics*, May/June (1988);

[44] A. Afanasev *et al.*, *Phys.Rev.D* **64**, 113009 (2001); *Phys. Lett. B* **514**, 269 (2001); *Phys. Rev. D* **65**, 013006 (2002). E03109

[45] G. Warren, O.A. Rondon, JLab E01-109, Spin Asymmetries on the Nucleon Experiment (SANE)

[46] T.W. Donnelly and A.S. Raskin, Annals of Phys., 169, 247 (1986).

[47] G. Warren, G_{Ep}/G_{Mp} via Simultaneous Asymmetry Measurements of Reaction $\vec{p}(\vec{e},e')$, proposal to JLab PAC-20.

[48] Report of the July 17-20, 2001 Meeting of the Jefferson Lab Program Advisory Committee PAC 20.